Overview of the JT-60SA Project

S. Ishida[1)], P. Barabaschi[2)], Y. Kamada[3)] and the JT-60SA Team

1) JT-60SA Project Team and 3) JT-60SA JA-Home Team, Japan Atomic Energy Agency, 801-1 Mukoyama, Naka, Ibaraki, 311-0193 Japan, 2) JT-60SA EU-Home Team, Fusion for Energy, Boltzmannstr 2, Garching, 85748, Germany

E-mail contact of main author: ishida.shinichi@jaea.go.jp

Abstract. This paper overviews the achievements and plans of the JT-60SA project which has been implemented jointly by Europe and Japan since 2007, covering the objectives, performance, schedule, design and procurement activities and on-site preparations. Re-baselining of the project was completed in late 2008, where all the scientific missions are preserved with the newly designed machine to meet the cost objectives. The construction of the JT-60SA has began with procurement activities for components of the toroidal field magnet, poloidal field magnet, vacuum vessel, in-vessel components, cryostat, power supplies under the relevant procurement arrangements between the implementing agencies of Japan Atomic Energy Agency in Japan and Fusion for Energy in Europe in parallel with dismantling the JT-60 facilities, at the end of which the first plasma is foreseen in 2016. For exploitation, development of the JT-60SA research plan has been started jointly between Japan and Europe.

1. Introduction

Construction and exploitation of the JT-60SA (JT-60 Super Advanced) are being implemented at the Japan Atomic Energy Agency (JAEA) Naka site in Japan under the Satellite Tokamak Programme, to be undertaken as part of the Broader Approach (BA) agreement jointly implemented by Europe and Japan from June 2007, and the Japanese national programme. The mission of the JT-60SA project is to contribute to the early realization of fusion energy by supporting the exploitation of ITER and research towards DEMO by addressing key physics issues associated with these machines as shown in Fig.1 [1].

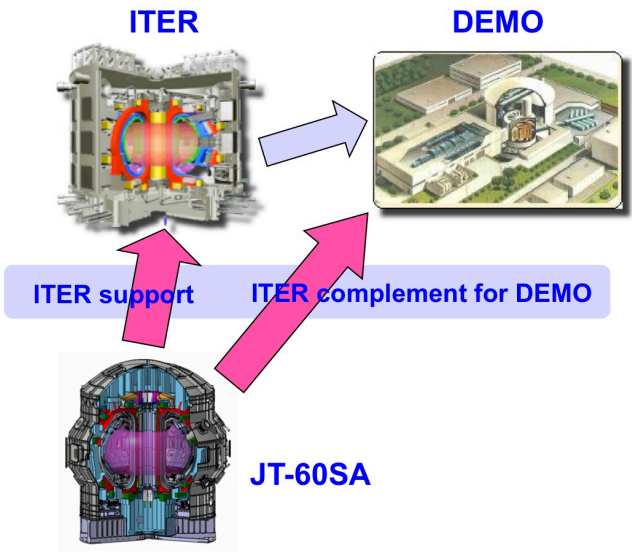

Fig.1 Schematic view of the mission of the JT-60SA project

The JT-60SA will be capable of confining break-even equivalent class high-temperature deuterium plasmas at a plasma current I_p of 5.5 MA, a major radius of ~3 m and a toroidal field of 2.25 T lasting for a duration longer of ~100 s than the timescales characteristic of plasma processes such as current diffusion, pursue full non-inductive steady-state operation with high plasma beta close to and exceeding no-wall ideal stability limits, and establish ITER-relevant high density plasma regimes well above the H-mode power threshold [2]. High β_N regime to be pursued is shown with possible DEMO and ITER regimes in Fig.2.

Re-baselining of the project has been prompted by cost concerns and developed intensively since late 2007. The re-baselining was completed in late 2008, in which the newly designed machine preserves all the scientific missions for the JT-60SA project and is expected to meet

its cost objectives[1,2,3]. The re-baselining also complies with additional design requirements and adds further flexibility features. In accordance with Procurement Arrangements (PAs) concluded between Fusion for Energy and JAEA, manufacturing activities have commenced in 2009 with new facilities for superconducting coils at the Naka site and development of a prototype for the vacuum vessel on the manufacturing factory. Up to date, eleven PAs have been concluded, following which the procurement activities have been implemented for the supply of the Toroidal Field (TF) magnet, Poloidal Field (PF) magnet, vacuum vessel, in-vessel components of divertor cassettes and first wall materials, cryostat, power supplies. According to the PAs, industrial contracts have been launched when in place. The JT-60SA project has already undertaken construction activities for completion of the new machine as discussed in the present paper.

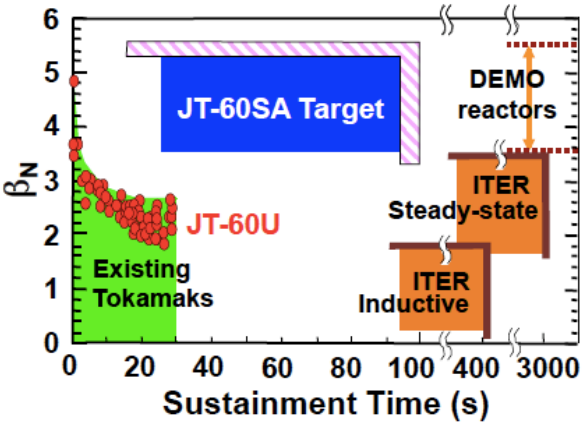

Fig.2 High β_N target regime of JT-60SA

2. Performance and Design Requirements

The JT-60SA project set out the following technical objectives including specification targets in order to accomplish the mission with maximum utilization of the integrated and outstanding machine capabilities for which none of those of existing tokamaks can be substituted as follows;

Plasma performance:

- The device should be capable of confining break-even equivalent class high-temperature deuterium plasmas (equivalent Q_{DT} around unity) lasting for a duration longer than the timescales characteristic of plasma processes.
- The device should pursue full non-inductive steady-state operation with high plasma beta close to and exceeding no-wall ideal stability limits.
- The device should establish ITER-relevant high density plasma regimes well above the H-mode power threshold.

Design requirements:

- In order to satisfy the above plasma performance requirements, the machine design should be able to support a wide range of plasma equilibria with divertor configurations covering a high plasma shaping factor of S~6 and a low aspect ratio of A~2.5.
- In order to satisfy the above plasma performance requirements, an inductive plasma current flattop and additional heating up to 41 MW during 100 s, under nominal operating conditions, should be provided.
- In order to allow the high heat and particle fluxes to the divertor, the divertor target should stand up to 15 MW/m^2.
- In order to pursue full non-inductive steady-state operation, negative-ion based neutral beam injection (N-NBI) with high beam energy up to 500 keV should be provided.
- In order to sustain high plasma beta exceeding no-wall ideal stability limits, internal resistive-wall-mode (RWM) stabilizing coils should be equipped with stabilizing shell.

- In order to allow in-vessel maintenance necessary for experimental campaigns with high-power and/or long-pulse operation of deuterium plasmas, in-vessel components should be equipped to be compatible with remote maintenance.
- The choice of machine parameters and functional specifications of the components for the device should be consistent with the required plasma performance and design requirements and made to meet the cost objectives.

3. Machine Parameters and Components

In order to satisfy the above requirements, the machine has been coherently re-designed to cover: a wide range of plasma equilibria with divertor configurations covering a higher plasma shaping factor of S~6.7, a lower aspect ratio of ~2.5, a high triangularity of δ_x~0.53, and a high elongation of κ_x~2.0; an inductive plasma current flattop and additional heating up to 41 MW during 100 s; divertor targets to stand up to 15 MW/m^2; N-NBI with high beam energy up to 500 keV; in-vessel coils for RWM stabilization equipped with stabilizing shell; in-vessel components such as divertor cassettes to be compatible with remote maintenance. The design integration of the machine has been completed as the new machine with basic parameters as shown in Fig.3 and Table 1.

Table 1: Basic parameters of JT-60SA

Plasma Current	5.5 MA
Toroidal Field, B_t	2.25 T
Major Radius, R_p	2.96
Minor Radius, a	1.18
Elongation, κ_X	1.95
Triangularity, δ_X	0.53
Aspect Ratio, A	2.5
Shape Parameter, S	6.7
Safety Factor, q_{95}	~3
Flattop Duration	100 s
Heating & CD Power	41 MW
N-NBI	10 MW
P-NBI	24 MW
ECRF	7 MW
Divertor wall load	15 MW/m^2

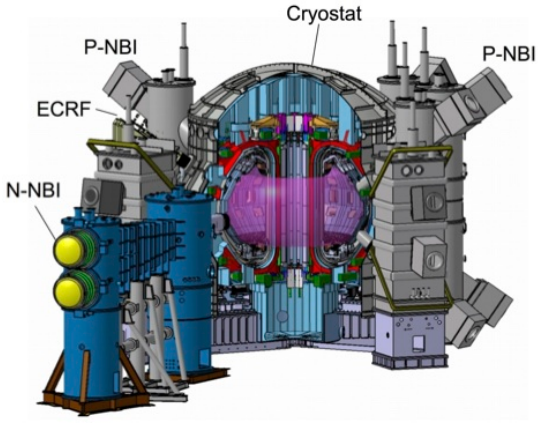

Fig.3 Cross-section of the JT-60SA tokamak

The cross-section of the JT-60SA tokamak is shown in Fig.4. The superconducting magnet system consists of 18 Toroidal Field (TF) coils, a Central Solenoid (CS) with four modules, 6 Equilibrium Field (EF) coils. Each TF coil uses a rectangular steel-jacketed NbTi cable-in conduit conductor. The PF magnet is composed of the CS and EF coils using Nb_3Sn and NbTi cable-in conduit conductors, respectively. The vacuum vessel (VV) uses low cobalt SS to reduce activation levels. The divertor consists of inner and outer vertical targets with a V-shaped corner. Cryopanels will be installed below the divertor cassette for particle control. Three sets of copper coils consisting of a pair of fast plasma position control coils, 12 error field correction coils and 18 RWM

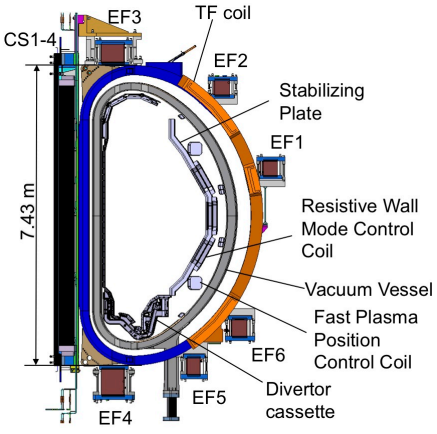

Fig.4 Cross-section of the JT-60SA tokamak for the initial research phase

control coils will be installed inside the VV. The cryostat consists of a vessel body and a base used for the gravity and seismic support of the machine. Other components such as power supplies, cryogenic system, N-NBI/Positive ion NBI (P-NBI)/ECRF systems have also been consistently designed.

The JT-60SA will be build jointly by Europe and Japan at the Naka site. Sharing of in-kind contributions by Japan and Europe, including those procured by the Japanese national program, is schematically illustrated in Fig.5. Existing JT-60 facilities will also be utilized. In Europe, with some parts directly contributed by Fusion for Energy, the procurement is being also carried out by the EU Voluntary Contributors which participate to the BA activities: CEA in France (cryogenic system, TF magnet, power supplies, TF coil test), ENEA (TF magnet, power supplies, TF coil test) and Consorzio-RFX (power supplies) in Italy, KIT (high-temperatue superconducting current leads) in Germany, CIEMAT (Cryostat) in Spain, SCK-CEN(TF coil test) in Belgium.

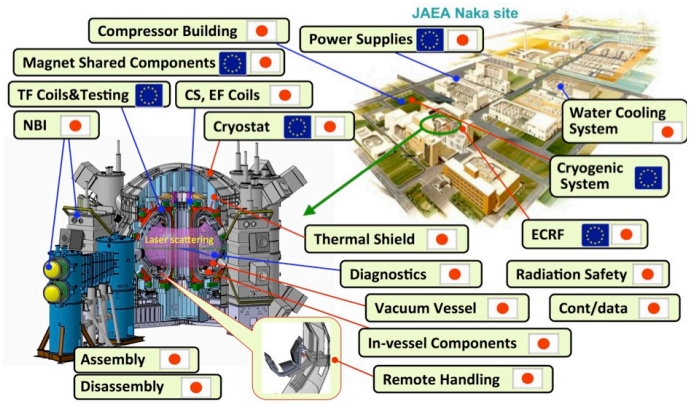

Fig.5 Sharing of contributions from Europe and Japan for JT-60SA

4. Operation Scenarios

Reference operation scenarios have been designed as referred to [4]. A reference scenario is shown in Fig.6, where the temporal evolutions of the CS3 coil current and the plasma current and the corresponding equilibrium are indicated.

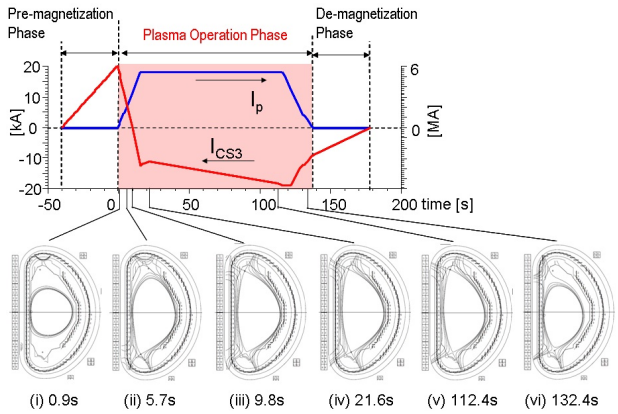

Fig.6 Reference operation scenario for a double null discharge with 5.5 MA

The plasma performance was assessed, so that it was confirmed that all the scientific missions can be achieved as specified in the above requirements as follows;

i) A shaping controllability is obtained thanks to a lower aspect ratio, A=2.5, for Lower Single Null (LSN) and Double Null (DN) configurations showing κ_x=1.87(1.95), δ_x=0.50(0.53) and S=6.3(6.7) for LSN (DN) at q_{95}~3, where S is the shape factor defined by $S = q_{95}I_p[MA]/a[m]Bt[T]$.

ii) A high fusion triple product of (5-7)×10^{20} m^{-3}•s•keV with I_p=5.5 MA, f_{GW}=0.8 and HH_{98y2} =1.1-1.3, is expected to be produced, where f_{GW} is the ratio of average density to the Greenwald density. In these plasmas, the density at f_{GW}=0.8 is 1×10^{20} m^{-3}, namely ITER-relevant, while the threshold power for L to H transition (P_{LtoH}) is 15 MW.

iii) As for non-inductive steady-state operation, high β_N plasmas are expected to be fully non-inductively driven; I_p=2.3 MA, B_t=1.72 T, q_{95}=5.8, f_{GW}=0.85, f_{BS}=0.68, β_N=4.3,

HH_{98y2}=1.3, P_{heat}=37 MW (20 MW of N-NB, 10 MW of P-NB and 7 MW of ECRF), where f_{BS} is the bootstrap current fraction.

iv) The divertor performance is simulated by using the SONIC code for the newly designed lower divertor. The peak heat load q_{peak} is expected to be maintained less than 11 MW/m^2 by gas puffing (1.5×10^{22} s^{-1} or 30 Pam^3/s) for 41 MW, 4 MW of which is assumed to be radiated in the main plasma core.

5. Schedule

5.1 Construction Phase

The high-level project schedule is shown in Fig.7, which was approved by the Broader Approach Steering Committee with the completion of the re-baselining in late 2008 taking into account a more detailed analysis of the manufacturing and assembly schedule as well as the delay incurred by the project due to the re-designing of the machine. As a result, the milestone of "First Plasma" is foreseen in 2016. Other main milestones are set out as "Start Tokamak Assembly" in 2012, "Complete Tokamak Assembly" in 2015.

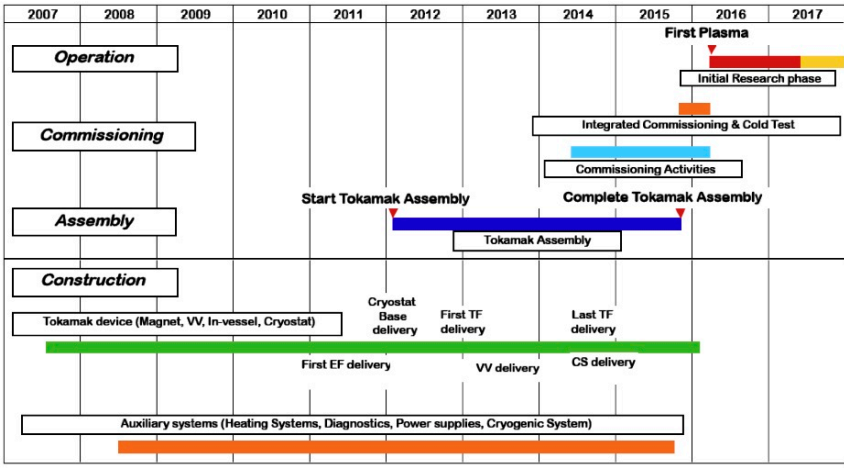

Fig.7 High-level project schedule for JT-60SA

5.2 Operation Phase

The JT-60SA facilities will be upgraded step by step according to the phased operation plan as shown in Table 2, where the operational phase is correspondingly shown as an initial research phase (hydrogen phase and deuterium phase), an integrated research phase, and an extended research phase.

Table 2: Operation phases and status of key components

	Phase	Expected Duration		Annual Neutron Limit	Remote Handling	Divertor	P-NB	N-NB	ECRF	Max Power	Power x Time
Initial Research Phase	phase I	1-2 y	H	-	R&D	LSN partial monoblock	10MW	10MW	1.5MW x100s + 1.5MW x5s	23MW	NB: 20MW x 100s 30MW x 60s duty = 1/30 ECRF: 100s
	phase II	2-3y	D	4E19			Perp. 13MW Tang. 7MW			33MW	
Integrated Research Phase	phase I	2-3y	D	4E20		LSN full-monoblock			7MW	37MW	
	phase II	>2y	D	1E21	Use						
Extended Research Phase		>5y	D	1.5E21		DN	24MW			41MW	41MW x 100s

A JT-60SA research plan is being developed in which a staged approach will be employed consistently with the phased upgrade in machine capability as discussed above. Based on

scientific achievements in the world devices, a consistent set of research objectives and strategy covering all the major research fields is being considered as follows; i) operation regime development, ii) MHD stability and control, iii) transport and confinement iv) high energy particle behavior, v) edge and pedestal characteristics, and vi) divertor, scrape off layer (SOL) and plasma material interaction (PMI) [4].

6. Design Integration

A single distributed organization put in place for the international implementation of the project is depicted as an "Integrated Project Team", built by the union of the Project Team, the EU Home Team, and the JA Home Team, to execute the project. Since design activities for each component are made in distributed institutes in Europe and in Japan, design integration, or configuration and interface management, is key for the project. The principle of configuration and interface management is that all aspects of technical information describing interfaces are elaborated, to the extent necessary in order to define the scope of supply of each system and make sure that systems match each other.

To this effect, one single document, named Plant Integration Document (PID), is developed and maintained by the whole team to provide all the latest information necessary to understand the requirements, configuration and interfaces of the JT-60SA machine. The PID includes or refers to all interface information as structured by the system design, parameters and requirements of each system, WBS(Work Breakdown Structure)/PBS(Plant Breakdown Structure), interface scope of supply sharing, and glossary. The PID is subject to change control at the Technical Coordination Meeting, in accordance with the JT-60SA Common Quality Management System. The PID is updated typically a few times per year in order to include evolution of design and interface information.

7. Design and Procurement Activities

The machine design and the procurement activities including upgrading of existing facilities are outlined as follows and the design evolution is detailed in [3].

7.1 Superconducting Magnet

The superconducting magnet system is shown in Fig.8[5]. High Temperature Superconductor (HTS) current leads (CLs) will be used to reduce cryogenic load and operational cost. The PAs for the supply of the PF magnet, HTS-CLs and TF magnet have been launched in 2007-2010.

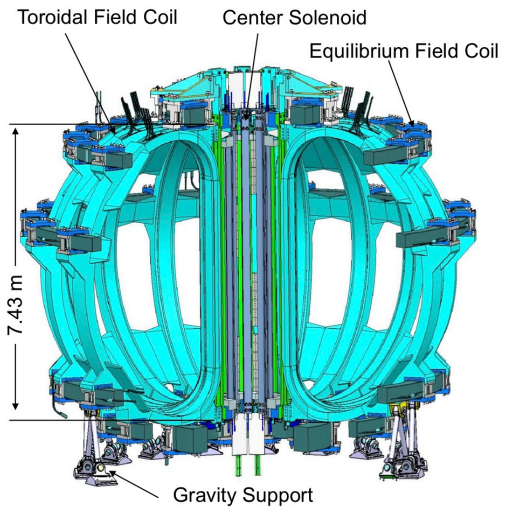

Fig.8 Assembly of the superconducting magnets

The TF magnet is built by an assembly of 18 coils. Each TF coil has a D-shaped form and is wound from a rectangular steel-jacketed NbTi cable-in conduit conductor which is cooled by a forced-flow of supercritical helium. The TF coils conductor is a Cable-In-Conduit Conductor (CICC) which relies on twisted, multi-filament NbTi composite strands. The winding package uses one-in-

hand configuration of six double pancakes, each pancake having six turns. The winding pack is inserted in a stainless steel casing. The superconducting strand and conductor specifications were qualified through three samples produced and tested between 2008 and 2009 in the SULTAN facility at CRPP in Switzerland. The TF conductor design was found sound with respect to the temperature safety margin (at least 1 K).

The coils are wedged together over their straight section to support the in-plane centralising forces. Overturning moments on the coils are supported by dowels between the casings in the upper and lower inboard curved regions, and this region is pre-compressed by toroidal bolts during assembly. The Outer Intercoil Structure (OIS) consists of 18 sections. Bolted shear plates, with friction surfaces and intermediate insulation, form a complete structure to house the full magnet and support the out of plane loads. The TF coil casing is supported by a gravity support which is bolted to the cryostat ring. The gravity support of each coil is enveloped in a thermal shield and includes a cryogenically-cooled thermal barrier. The plans of contracts for strand, cabling and jacketing, winding, coil manufacturing are detailed in [5].

The CS is a vertical stack consisting of four independently winding pack modules. The stack is hung from the top of the TF coils through flexible supports and is provided at the bottom with a locating mechanism which acts as a support against dynamic horizontal forces. The CS pre-load structure, which consists of a set of tie plates located outside and inside the coil stack, provides axial pressure on the stack. The CS stack is self-supporting against the coil radial forces and most of the vertical forces, with the support to the TF coil reacting only the weight and net vertical components resulting from up-down asymmetry of the poloidal field configuration. The winding configuration of the CS was changed from Hexa(6)-pancake to Octa(8)- pancake so to reduce the number of pancake joints. The six EF coils are attached to the TF coil cases through supports which include flexible plates allowing radial displacements. The PF coils are optimized to provide suitable magnetic fields for the plasma equilibrium and control and their position and size have been optimized accordingly, within the constraints imposed by the access to the in-vessel components.

As shown in Fig.9 and Fig.10, two new buildings were completed at the Naka site in 2009. One is the superconducting coil winding building (W 25 m, L 80 m, H 11 m) for winding all the EF coils from EF1 to EF6, where series production of the conductors are on-going. Another is the jacketing building (W 15 m, L 38 m, H 9 m, with a jacketing line 630 m) for jacketing the superconducting cables of the central solenoid (CS) and the EF coils.

Fig.9 Manufacturing of EF conductors with a 630 m jacketing line at the JAEA Naka Site in May 2010

Fig.10 PF coil manufacturing building with a 80 m long which was completed at the JAEA Naka site in March 2009

7.2 Vacuum Vessel

The new VV of JT-60SA is composed of 18 toroidal sectors constructed out of SS316L with low cobalt content of < 0.05 wt%, to reduce activation levels as shown in Fig.11[6]. The overall vessel parameters are the torus inside and outer diameter of 2.86 m and 9.95 m, respectively, and the torus hight of 6.63 m, the main vessel body weight of ~150 ton and one turn resistance of ~16 μΩ. The inner shell has a multi-arced shape in the poloidal direction and 36 facets (10 degree segments) in the toroidal direction. The outer shell shares the same arcs in the poloidal direction but has a slightly different faceting pattern that follows the presence of ribs. Seismic waves and response spectra of seismic motion at the ground floor of the JT-60 building for the design basis earthquake motion S1 were evaluated based on the previous works for ITER site selection on Naka-site and the JT-60SA seismic analysis. Based on this result, the VV gravity support with 9 legs is designed with the rigidity of the laminated leaf spring and the joint against the seismic motion of 1 G.

The flow of boric acid water (boron water) between shells was retained for neutron shielding reasons with some increase in the thickness of the boron-water layer to provide sufficient neutron shielding performance considering the thickness of TF coil case. The vacuum vessel can be baked up to 200°C using nitrogen gas after draining the borated water. Baking at 200°C will be done to keep the Thermal Shield at 100 K. This temperature is required to allow a matching of the refrigeration loads with the plant capacity for normal operation. The temperature of the vacuum vessel in normal operation is kept at ~50°C. The inlets of the water and nitrogen gas are located in the lower region of the vessel body.

In accordance with the PA for the VV concluded in 2008, development of a trial upper half of the 20 degree sector of the VV has been completed in 2010 to allow series production of the VV, where welding processes are successfully finished as shown in Fig.12.

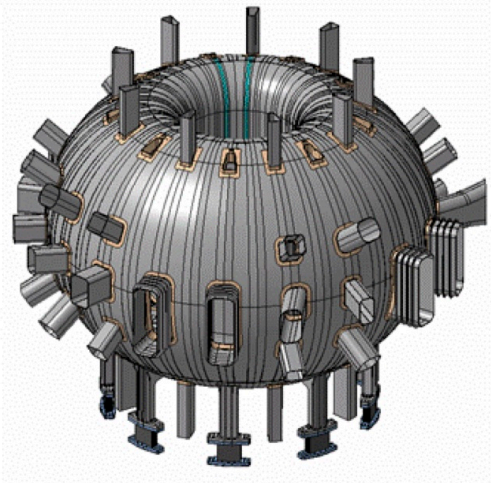

Fig.11 Vacuum vessel and ports

Fig.12 Trial upper half of the 20 degree sector of the vacuum vessel was delivered to the Naka site

7.3 Invessel Components

The divertor consists of the inner and outer vertical targets with a V-shaped corner for the outer one to enhance particle recycling and reduce target heat flux, a private flux region dome, the inner and outer baffles capable of withstanding a medium heat flux, and a divertor cassette body as shown Fig.13[7]. Cryopanels will be installed between the divertor cassette and the

VV as divertor pumping for particle control. Cooling water pipes will be also installed in the VV. The design of the lower divertor cassette, which will be initially installed, is optimized so as to obtain a higher plasma triangularity for a LSN configuration.

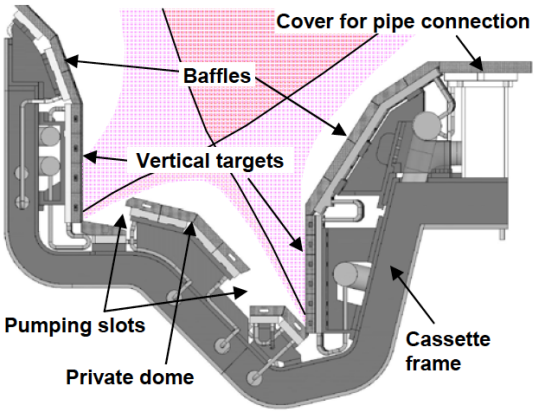

Fig.13 Cross-section of the divertor cassette for a lower single null divertor in the initial research phase.

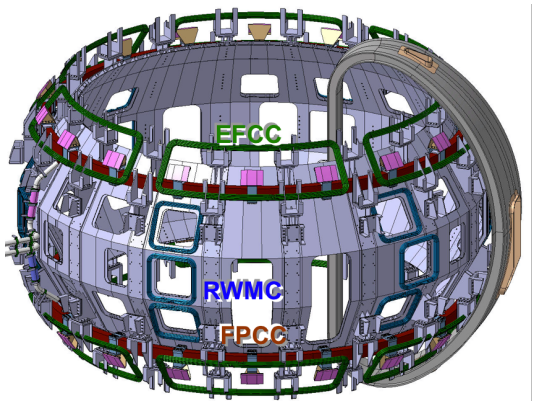

Fig.14 assembly of the RWM coils(RWMC), fast plasma position control coils(FPCC) and error field correction coils(EFCC) on the stabilizing plates to be installed in the vacuum vessel.

A combination of bolted CFC targets for most of cassettes and CFC monoblock targets for a few cassettes will be used for the initial research phase, while the former will be exchanged to the monoblock targets in a later phase in order to allow high heat flux (up to 15 MW/m^2) operation lasting for 100 s. 12 full-size mock-ups of the monoblock target to examine brazing for the target were manufactured and the performance has been tested by cyclic heat load test using the JEBIS (JAEA Electron Beam Irradiation Stand) facility[7]. The divertor cassettes are also designed to be compatible with remote handling maintenance for the preparation of future increase in radioactivation. The inner and outer first wall will be covered with bolted armour tiles on cooled heat sink. Bolted graphite tiles on cooled heat sink withstand the heat flux of 0.1-0.3 MW/m^2 for ~100 s. All plasma-facing components including the divertor target, baffle plates and inner/outer first wall will be water-cooled at 40°C. CFC materials at the first and second stages have been delivered in 2009 and 2010, respectively.

Three sets of water-cooled copper coils are shown in Fig.14. The fast plasma position control coils are situated between the VV and the stabilizing plate for control of vertical instability and position of high beta plasmas. The RWM control coils are needed to achieve steady state high beta plasmas. The error field correction coils will be used to eliminate the cause to destabilize the RWM, to ease plasma break down and avoid locked modes, and to control ELMs. Assessment for these in-vessel coils is discussed including disruption effects in [8].

7.4 Cryostat

The newly designed cryostat consists of a vessel body and a base used for the gravity and seismic support of the machine as shown in Fig.15. The lower cryostat base is much heavier in construction as it must bear the load of the entire machine and transmit gravity and seismic loads to the lower pillars below the floor of the torus hall. The base consists of two rings connected to the corresponding embedded ones below the floor level, 9 radial supports, a large double ring where the TF and VV supports are located and an inner cylindrical shell.

Seismic analyses indicate relatively low stress levels. The PA for the cryostat base, which will be the first deliverable from Europe to Japan, has been launched in 2009.

The actual vessel body of the cryostat is formed by cylindrical sections connected by truncated-conical elements in the inclined port sections. The top lid will be built with a torospherical shape in order to obtain enough room for the assembly and maintenance of the cryogenic devices such as in-cryostat feeder, insulation break and TF coil terminal joints. The vessel body will be made of single-wall stainless steel shell with a thickness of probably 34 mm. This single wall is externally reinforced with ribs to support the weight of all the ports and port plugs and also to withstand the vacuum pressure. The operational pressure is 10^{-3} Pa and the material SS 304 (Co<0.05 wt %). The load combination with dead weight, seismic loads, electromagnetic forces and thermal loads are taken into account for the structural design [9].

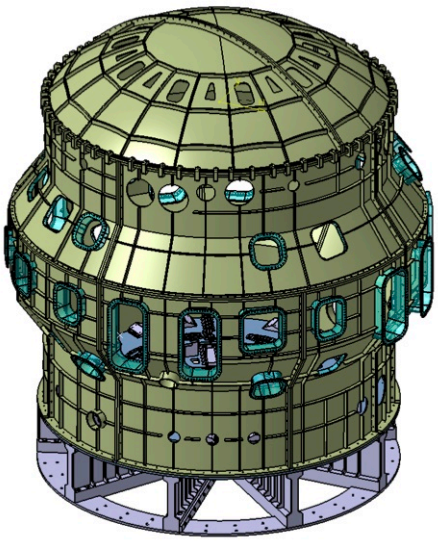

Fig.15 Assembly of the cryostat base and cryostat body

7.5 Cryogenic System

The cryogenic system is designed to provide refrigeration capacity for the thermal shields of the cryostat, the HTS-CLs, the superconducting magnet system and the divertor cryo-pumps. Different thermal shields around the vacuum vessel, the ports, the cryostat, and the distribution boxes as well as the Chevron baffles of the cryo-pumps are cooled to between 80 K and 100 K. A flow of supercritical helium at 4.4 K and 0.5 MPa is circulated through the superconducting coils, feeders and the cold structures. In addition, refrigeration capacity at 3.7 K is provided for the panels of the divertor cryo-pumps. The HTS-CLs require helium cooling to between 50 K and 300 K [10].

In 2008 and 2009 two studies were performed to analyze in detail the refrigeration process. As part of these studies, the major components were dimensioned and a new layout of the cryogenic system was proposed. All major interfaces with the site are defined and estimates for the utilities, investment and operation cost have been provided.

7.6 Power Supplies

AC power supply system will be reused without significant modification from the initial to the integrated research phase where heating power of 30 MW for 60 s or 20 MW for 100 s is planned. It is herein assumed that the H-MG (400MVA/2.6 GJ) will provide both real and reactive power to all poloidal field coil power supplies as requested by the reference operational scenarios including the plasma breakdown phase. The H-MG is also to transfer 20 MW of electricity to P-NBI with assist of continuous motor drive. Each 40 MW of P-NBI and N-NBI (80 MW power demand in total) will be delivered by T-MG (215 MVA/4.0 GJ) with continuous motor driving during plasma operation. 28 MW for ECRF will be directly

transferred from the 275 kV commercial power grid. For the toroidal field coil power supply, an existing 11 kV line with harmonic filters will be utilized.

DC power supply consists of the superconducting and in-vessel normal conductor coil power supplies. Many components of DC power supply for superconducting coils will be newly procured including thyristor converter, crowbar, Quench Protection Circuit (QPC) and switching network unit, while transformers of converter for Booster Power Supply are reuse components[11]. The PA for the QPC has been launched in 2010. The preliminary design of the fast plasma position control coil power supply has been completed in 2010.

7.7 ECRF System

For the initial research phase, 3 MW of RF power at 110 GHz will be injected into the plasma by 4 gyrotrons of 1MW each. Existing two gyrotrons and their power supplies, used on JT-60U, will be operated as a 5 sec system as they are. Two 1 MW gyrotrons at 110 GHz and two power supplies will be combined to provide the 100 s system. Two antennas will be installed and four waveguides will be modified partly using waveguides in JT-60U by Japan. As a result, 3 MW injection up to 5 sec by 4 gyrotrons will be expected for plasma initiation, and 1.5 MW injection up to 100 s by 2 gyrotrons will be expected for ECH/CD [12].

For the integrated research phase, two of the 5 sec units in the initial research phase will be upgraded to 100 sec units. Five additional 110 GHz gyrotrons and power supply sets will be fabricated and installed. Two additional antennas for five waveguides will be fabricated and installed. As a result, 7 MW (at 110GHz) will be injected to the plasma for 100 sec by 9 gyrotrons of 1 MW, assuming a transmission efficiency of 0.75-0.8.

7.8 NBI System

The NBI system to be upgraded for JT-60SA consists of twelve positive-ion-based NBI (P-NBI) units and one negative-ion-based NBI (N-NBI) unit[13]. The beam line of the co-tangential N-NBI unit is shifted downward from the equatorial plane by ~0.6 m to drive off-axis plasma current, and hence to produce a reversed shear profile with a high bootstrap current fraction.

Recent development of the N-NBI has shown that voltage resistance of ion source was remarkably improved by optimizing the electrode spacing: i) inter-electrode distance was widened based on the newly acquired voltage-resistance characteristics for large electrodes (ϕ160cm), ii) this optimization ensures good beam convergence as well. As a result, H^- beam of 500keV/3A (WR) was stably produced to meet the requirement in JT-60SA.

8. Disassembly of JT-60 Facilities

Since the torus hall has to be cleared in 2012 to launch the tokamak assembly in the torus hall following the delivery of the cryostat base from Europe. The disassembly activities at the JAEA Naka site proceed on schedule, which started in 2008 including land preparation of temporal storage areas in the Naka site.

In the JT-60 assembly hall, removing components such as the high-voltage bushing of the N-NBI, support structures for the ion sources and the high-voltage table of the N-NBI, started from November in 2009 and was completed in January 2010. Disassembly of the neutron

shield wall started in February and was completed at the end of March. Diagnostic apparatus installed in and on the diagnostic stage in the torus hall was disassembled and removed beforehand, and the diagnostic stage itself, 40 m in length and 200 t in weight, was removed from the torus hall to the assembly hall. These series photos in the hall are shown in Fig.16.

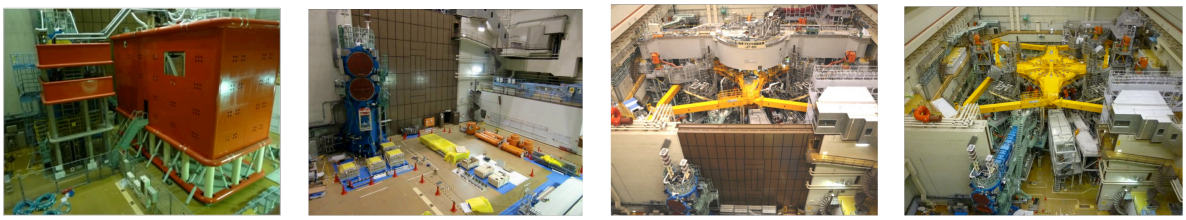

Fig.16 Progress in disassembly in the JT-60 torus hall

9. Conclusions

After successful completion of the re-baselining in late 2008, the project has made a large progress in designing, manufacturing, planning and site preparation towards the start of the JT-60SA tokamak assembly in 2012 and the first plasma in 2016. The procurement implementation for the components has progressed including industrial contracts in accordance with the concluded PAs for the supply of the PF magnet, vacuum vessel, divertor and first wall materials by Japan and the power supply, cryostat, HTS-CLs and TF magnet by Europe. Manufacturing activities have commenced with building new facilities for the PF coils at the JAEA Naka site and development of a prototype for vacuum vessel has been completed and delivered to the Naka site in 2010. Disassembly of the JT-60 faculties proceeds on schedule at the Naka site. The development of JT-60SA research plan has already started jointly between EU and JA for future exploitation in JT-60SA.

Acknowledgement

The main three authors wish to thank all the JT-60SA Team members for their dedicated contributions to this project.

References

[1] S. Ishida et al., to be published in Fusion Engineering and Design.
[2] Y. Kamada et al., Journal of Plasma and Fusion Research SERIES Vol. 9 (2010) 641.
[3] P. Barabaschi et al, this conference, FTP/2-1.
[4] Y. Kamada et et al., this conference, FTP/P6-04.
[5] M. Peyrot et sl, this conference, FTP/P6-29.
[6] S. Sakurai et al., Fusion Engineering and Design, **84**, (2009), 1684.
[7] S. Sakurai et al, this conference, FTP/P1-29.
[8] M. Takechi et al, this conference, FTP/P6-30.
[9] Y.K. Shibama et al., Fusion Engineering and Design, **83**, (2008), 1605.
[10] P. Roussel, et al., to be published in AIP Conf. Proc. (2010).
[11] El. Gaio, et al., Fusion Engineering and Design, **84**, (2009), 804M.
[12] S. Moriyama, et al., 34th Int. Conf. on Infrared, Millimeter and Terahertz Waves, (2009).
[13] Y. Ikeda, et al., IEEE Transactions on Plasma Science, **36**, (2008), 1519.

The JT-60SA Team

N. Akino[1], J. Alonso[2], T. Arai[1], F. Ardellier[3], S. Asakawa[1], N. Asakura[1], D. Balaguer[4], P. Barabaschi[5], G. Barrera[2], O. Baulaigue[6], P. Bayetti[6], U. Besi[7], T. Bolzonella[8], J. Botija[2], P. Cara[5], M. Chantant[6], P. Chesny[3], S. Chiba[1], R. Coletti[7], A. Coletti[5], B. Collins[9], V. Corato[7], P. Costa[7], A. Cucchiaro[7], A. Dael[6], S. Davis[5], P. Decool[6], A. Della Corte[7], C. Delrez[9], A. Di Zenobio[7], E. Di Pietro[5], G. Disset[3], H. Dougnac[6], J-L. Duchateau[6], D. Duglue[5], Y. Endo[1], P. Fernandez[2], A. Ferro[8], W. Fietz[10], T. Fujita[1], M. Fukumoto[1], E. Gaio[8], L. Genini[3], A. Geraund[6], P. Gouat[9], G. Gros[4], N. Hajnal[5], K. Hamamatsu[1], T. Hamano[1], M. Hanada[1], K. Hasegawa[1], T. Hatae[1], N. Hayashi[1], T. Hayashi[1], R. Heller[10], P. Hertout[6], S. Higashijima[1], J. Hinata[1], S. Hiranai[1], D. Hitz[4], C. Hoa[4], A. Honda[1], M. Honda[1], R. Hoshi[1], Kat. Hoshino[1], Kaz. Hoshino[1], T. Ichige[1], H. Ichige[1], S. Ide[1], Y. Ikeda[1], A. Isayama[1], S. Ishida[1], Y. Ishige[1], K. Itami[1], P. Jametton[9], G. Jiolat[6], L. Jourdheuil[6], Y. Kamada[1], I. Kamata[1], A. Kaminaga[1], Ke. Kamiya[1], Ko. Kamiya[1], Y. Kashiwa[1], I. Kawai[1], Y. Kawamata[1], H. Kawashima[1], M. Kazawa[1], K. Kikuchi[1], S. Kitamura[1], K. Kiyono[1], K. Kizu[1], K. Kobayashi[1], T. Kobayashi[1], Y. Koide[1], A. Kojima[1], S. Kokusen[1], M. Komata[1], M. Komeda[1], T. Kominato[1], K. Komuro[1], H. Kubo[1], N. Kubo[1], M. Kuramochi[1], K. Kurihara[1], K. Lackner[5], B. Lacroix[6], V. Lamaison[4], Y. Maesaki[1], J. -L. Marechal[6], K. Masaki[1], V. Massaut[9], M. Matsukawa[1], H. Matsumura[1], G. Matsunaga[1], Y. Matsuzawa[1], M. Medrano[2], C. Melorio[7], L. Meunier[5], F. Michel[4], F. Millet[4], N. Miya[1], A. Miyamoto[1], Y. Miyo[1], K. Mogaki[1], F. Molinie[3], M. Mori[1], S. Moriyama[1], H. Murakami[1], A. Murofushi[1], L. Muzzi[7], O. Naito[1], S. Nakamura[1], T. Nakano[1], S. Nemoto[1], S. Nicollet[6], T. Nishiyama[1], L. Novello[8], H. Numata[1], F. Nunio[3], Y. Ohmori[1], Y. Ohnishi[1], K. Ohshima[1], M. Ohzeki[1], A. Oikawa[1], F. Okano[1], J. Okano[1], F. Orsitto[7], T. Oshima[1], N. Oyama[1], H. Ozaki[1], T. Ozeki[1], M. Peyrot[5], G. Phillips[5], A. Pizzuto[7], G. M. Polli[7], J-M. Poncet[4], P. Ponsot[3], C. Portafaix[6], F. Ramos[2], L. Reccia[7], B. Renard[3], P. Reynaud[6], E. Rincon[2], P. Roussel[4], H. Saeki[1], A. Sakasai[1], S. Sakata[1], T. Sakuma[1], S. Sakurai[1], A. Santagiustina[6], M. Santinelli[7], T. Sasajima[1], S. Sasaki[1], M. Sato[1], Mi. Sato[1], F. Sato[1], Y. Sato[1], M. Sawahata[1], H. Sawai[1], L. Scola[3], M. Seki[1], N. Seki[1], Y. K. Shibama[1], K. Shibanuma[1], K. Shibata[1], K. Shimada[1], K. Shimizu[1], T. Shimizu[1], M. Shimono[1], K. Shinohara[1], A. Soleto[2], B. Spears[5], F. Starace[7], M. Sueoka[1], T. Sugimura[1], A. M. Sukegawa[1], H. Sunaoshi[1],Takah. Suzuki[1], Takas. Suzuki[1], Mi. Suzuki[1], Ma. Suzuki[1], Hiroa. Suzuki[1],Hiros. Suzuki[1], S. Suzuki[1], M. Tabe[1], M. Takechi[1], T. Takizuka[1], T. Terakado[1], M. Terakado[1], B. Teuchner[5], H. Tojo[1], V. Tomarchio[5], A. Torre[4], T. Totsuka[1], K. Tsuchiya[1], Y. Tsukahara[1], S. Turtu[7], H. Urano[1], K. Usui[1], J. Vallet[4], C. Vanhille[3], J-M. Verger[4], M. Verrecchia[5], L. Vieillard[3], S. Villari[7], Ka. Wada[1], Ke. Wada[1], M. Wanner[5], E. Weiss[10], J. Yagyu[1], T. Yamaguchi[1], K. Yamauchi[1], K. Yokokura[1], M. Yoshida[1], K. Yoshida[1], L. Zani[5], C. Zignani[7]

Permanent addresses

[1] JAEA, Ibaraki, Japan
[2] CIEMAT, Madrid, Japan
[3] CEA, Grenoble, France
[4] F4E, Garching, Germany
[5] CEA, Cadarache, France
[6] CEA, Saclay, France
[7] ENEA, Rome, Italy
[8] Consorzio-RFX, Padova, Italy
[9] FZK, Karlsruhe, Germany
[10] SCK-CEN, Brussels, Belgium